pressure level is 1.0 dB higher with the ATW removed than with it in place. The data indicate that the ATW causes the 1.0 dB reduction almost uniformly over all the frequencies for which data were taken.

The small differences between the Configuration E data shown in Fig. 2 and that in Fig. 3 are due to experimental inaccuracy, some of which may be attributed to the fact that the two sets of data were taken on two different days. All of the data in Fig. 2 were taken on the same day; those in Fig. 3 were taken 11 days later.

V. The Possibility of a Laminar Boundary Layer Over an ATW Test Section

Although the design of a laminar inlet and test section of an aeroacoustic tunnel poses some problems, they seem to be of the kind that are easy to solve in principle and not too difficult in practice. As indicated[5] the amount of suction required to maintain a boundary-layer laminar is extremely small. According to Eqs. (17.5) and (17.6) in Ref. 5, the required suction velocity normal to the wall is no more than $-V_o = 1.2 \times 10^{-4} U_\infty$. For $U_\infty = 210$ fps $- V_o = 0.025$ fps. More suction than this will cause the boundary layer to become very thin. Equation (13.7) gives the displacement thickness $\delta^* = (\nu / V_o)$. Hence, if $V_o = -0.1$ fps, $\delta^* = 0.0016\ ft = 0.019\ in.$ From such relations it is found that the boundary layer is quite thin and the power required for suction is small.

This assumes uniform suction; an actual ATW will never be quite uniform, so more than the minimum required suction is needed. The suction could be provided in practice by pumping to reduce the pressure in the anechoic chamber that surrounds the ATW test section. The chamber pressure would need to be only very slightly less than the test-section static pressure. With some experimental development, such a facility might give a very quiet environment for aeroacoustic testing.

VI. Conclusions

A preliminary test of the ATW concept has been carried out, giving the following results: a) the ATW was very effective in improving the test-section flow as compared to that of an open jet. The boundary-layer development over the ATW was like that of a conventional wind tunnel, much thinner than the shear layer of an open jet; b) the ATW was effective in transmitting sound; only 1.0 dB transmission loss was incurred as compared to an open window; c) the four advantages of the ATW concept over the open-jet concept listed in Sec. I were all realized; however, some high-frequency noise was generated by the boundary-layer flow over the ATW; d) the ATW concept lends itself to the design of a tunnel test section with an all-laminar boundary layer. The boundary layer would be maintained in a laminar state by sucking test section air through the ATW into a surrounding anechoic chamber. Such an aeroacoustic tunnel might be made much quieter than any other tunnel if the suction airflowcan be kept at a low velocity and hence quiet.

References

[1] Patterson, R. W., Vogt, P. G., and Foley, W. M., "Design and Development of the United Aircraft Research Laboratories Acoustic Research Tunnel," *Journal of Aircraft*, Vol. 10, July 1973, pp. 427-433.

[2] Abramovich, G.N., *The Theory of Turbulent Jets*, The MIT Press, Cambridge, Mass., 1963.

[3] McCanless, G. F. and Boone, J. R., "Noise Reduction in Transonic Wind Tunnels," *Journal of the Acoustical Society of America*, Vol. 56, 1974, pp. 1501-1510.

[4] Bauer, A. B. and Chapkis, R. L., "Noise Generated by Boundary Layer Interaction with Perforated Acoustic Liners," AIAA Paper 76-41, Washington, D. C., Jan., 1976.

[5] Schlichting, H., *Boundary Layer Theory*, Pergamon Press, New York, 1955.

Design for Minimum Fuselage Drag

Jan Roskam* and Greg Fillman†
The University of Kansas, Lawrence, Kan.

Introduction

FUSELAGE drag in general aviation airplanes ranges from 30-50% of the total zero-lift drag of the airplane. It is important that the designer of such airplanes have a method for sizing the fuselage such that zero-lift drag is minimized under constraints of cabin volume (utility) and stability. This Note suggests such a method and shows that several existing general aviation airplane fuselages are not optimum from a drag viewpoint. Symbols used in this Engineering Note are defined in Ref. 1.

Discussion of Fuselage Fineness Ratio

Table 1 presents some data on fuselage fineness ratios for several current general aviation airplanes. It is interesting to note that with one exception, all have values of around $\ell_B/\mathrm{d} = 5$ to 6. In Ref. 1, the fuselage (or body) drag is estimated from

$$C_{D_{O_B}} = C_{f_B}\left[1 + \frac{60}{(\ell_B/\mathrm{d})^3} + 0.0025\left(\frac{\ell_B}{\mathrm{d}}\right)\right]\frac{S_{\text{wet body}}}{S_{\text{wing}}} \qquad (1)$$

This equation assumes zero base drag. Figure 1 shows how the [ ]-term in Eq. (1) is related to ℓ_B/d. Note that the [ ]-term no longer decreases significantly after $\ell_B/\mathrm{d} = 6.0$ is exceeded. This would indeed suggest that values of 5 to 6 for ℓ_B/d are about optimum. However, there are three other factors to contend with: 1) increasing ℓ_B/d will decrease C_{f_B} because of increasing Reynolds number; 2) increasing ℓ_B/d will increase $S_{\text{wet body}}$; and 3) increasing ℓ_B/d will decrease empennage wetted area requirements, for constant stability levels.

It appears that a more detailed examination of fuselage fineness ratio is therefore in order. The next section presents a method for minimizing the sum of fuselage and empennage friction drag, under constant directional and longitudinal stability constraints.

Minimizing General Aviation Airplane Fuselage and Empennage Zero-lift Drag

Fuselage Drag

It is assumed that the fuselage from nose to passenger compartment is defined roughly as in Fig. 2, and that this part of the fuselage is kept constant to satisfy volume and utility constraints. It is also assumed that the tail cone can be represented by a skewed cone as in Fig. 2. The equivalent fuselage diameter is defined as follows

$$\frac{\pi}{4}\mathrm{d}^2 = S_{\text{fus ref.}} \quad \text{so that} \quad \mathrm{d} = \left[\frac{4\,S_{\text{fus. ref.}}}{\pi}\right]^{1/2} \qquad (2)$$

The wetted area of the fuselage can now be written as

$$S_{\text{wet body}} = S_{\text{wet nose}} + S_{\text{wet cone}} = S_{\text{wet nose}} + F\cdot\pi\cdot\frac{\mathrm{d}}{2}\left[\left(\frac{\mathrm{d}}{2}\right)^2 + \ell_c^2\right]^{1/2} \qquad (3)$$

where F is a correction factor accounting for the fact that the rear fuselage is *not* a cone. F can be found by comparison to existing aircraft.

Received Sept. 22, 1975; revision received April 2, 1976.

Index categories: Aircraft Configuration Design; Aircraft Handling, Stability and Control; Aircraft Performance.

*Chairman and Professor of Aerospace Engineering. Associate Fellow AIAA.

†Undergraduate Research Assistant. Student Member AIAA.

Table 1 Examples of fuselage fineness ratios and wetted areas for general aviation aircraft

Type	ℓ_B/d	S_{wing}	$S_{wet\ body}$	$S_{wet\ body}/S_{wing}$
Cessna 210	5.02	175	319	1.82
Cessna 207	5.69	174	425	2.44
Beech Sierra	5.22	146	332	2.27
Cessna 185	5.15	176	292	1.68
Beech Bonanza ('58)	4.98	181	323	1.78
Beech Baron	5.69	199.2	362	1.82
Piper Navajo	5.97	229	502	2.19
Cessna 310	5.40	179	306	1.71
Piper Seneca	5.68	206.5	356	1.72
Beech Duke	5.59	212.9	586	2.28
Cessna 414	5.52	195.7	488	2.49
Beech King Air	6.06	294	652	2.22
Gates Learjet 24	8.8	232	502	2.16

The fuselage zero-lift drag coefficient can be expressed as

$$C_{D_{0_{fus}}} = C_{f_B}\left[1 + \frac{60}{(\ell_N+\ell_c)/d^3} + 0.0025\left(\frac{\ell_N+\ell_C}{d}\right)\right]\frac{S_{wet\ body}}{S_{wing}} R_{w_B} \quad (4)$$

Fuselage base drag is neglected. For given ℓ_C, $C_{D_{0_{fus}}}$ can thus be computed as a function of ℓ_c.

Empennage Drag

The horizontal tail wetted area may be approximated by

$$S_{wet_{H.T.}} = S_H\left(2 + \underset{\ll 1.0}{f(t/c)}\right) - C_{R_H}^2 \frac{d}{\ell_c} \quad (5)$$

where the geometry is defined in Fig. 2.

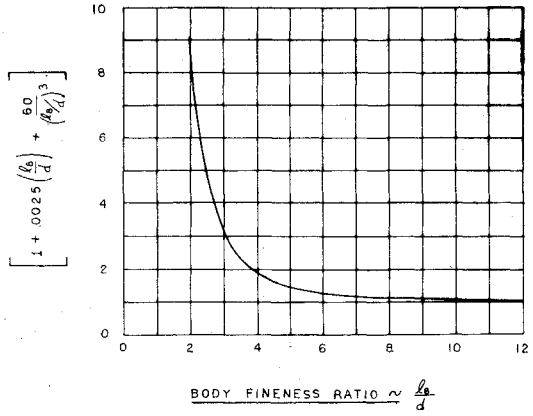

Fig. 1 Body zero-lift drag factor as a function of body fineness ratio.

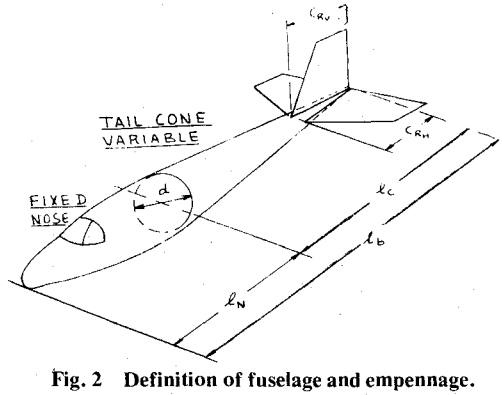

Fig. 2 Definition of fuselage and empennage.

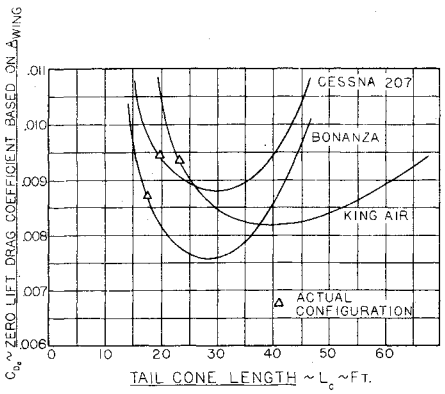

Fig. 3 Effect of tailcone length on fuselage plus empennage zero-lift drag under constant stability constraints.

The horizontal tail drag coefficient can be written as

$$C_{D_{0_{H.T.}}} = C_{f_H}\left[1 + L\left(\frac{t}{c}\right)_{H.T.} + 100\left(\frac{t}{c}\right)^4_{H.T.}\right] R_{L.S.} \frac{S_{wet\ H.T.}}{S_{wing}} \quad (6)$$

The vertical tail wetted area may be approximated by

$$S_{wet\ V.T.} = S_V\left(2 + \underset{\ll 1.0}{f(t/c)}\right) - \frac{1}{2} C_{R_V}^2 \frac{d}{\ell_c} \quad (7)$$

where the geometry is defined in Fig. 2.

The vertical tail drag coefficient can be written as

$$C_{D_{0_{V.T.}}} = C_{f_V}\left[1 + L\left(\frac{t}{c}\right)_{V.T.} + 100\left(\frac{t}{c}\right)^4_{V.T.}\right] R_{L.S.} \frac{S_{wet\ V.T.}}{S_{wing}} \quad (8)$$

Horizontal and vertical tail sizes are here assumed to be determined by minimum stability requirements, i.e.,: $C_{N_{\beta_{MIN}}}$ and $C_{m_{\alpha_{MIN}}}$.

Stability Constraints

By increasing the fuselage length, it is possible to lower the sizes of the vertical and horizontal tail. As a constraint, it is reasonable to assume that actual airplane C_{m_α} and C_{n_β} values should stay the same. Reference 2 gives formulas from which C_{m_α} and C_{n_β} can be expressed as functions of the variable aft fuselage geometry and horizontal and vertical tail sizes.

With the aid of the constant stability constraint it is possible to solve for S_H and $S_V l$. Using Eqs. (6) and (8) it is now possible to compute $C_{D_{0H}}$ and $C_{D_{0V}}$ as functions of $\ell_{B/d}$. By adding $C_{D_{0_{FUS}}}$ to $C_{D_{0_{H.T.}}}$ and $C_{D_{0_{V.T.}}}$ and plotting as a function of $\ell_{B/d}$ it is possible to find the minimum drag value of $\ell_{B/d}$ and the corresponding horizontal tail and vertical tail areas.

Example Calculations

The method suggested before was applied to three general aviation airplanes: The Beech King Air, the Beech Bonanza (V Tail), and the Cessna 207. Fig. 3 shows the results. It is seen that none of these airplanes are optimum with respect to this drag minimization method. The drag count differences of Fig. 3 are significant. They represent from 3 to 5% of the zero-lift drag of the example airplanes. It is possible to extend this method to include the effect of weight, and to include other stability and control constraints.

References

[1] Roskam, J., "Methods for Estimating Drag Polars of Subsonic Airplane," Roskam Aviation and Engineering Corporation, Lawrence, Kansas, 1972.

[2] Roskam, J., "Methods for Estimating Stability and Control Derivatives of Conventional Subsonic Airplanes," Roskam Aviation and Engineering Corporation, Lawrence, Kansas, 1972.